

ENHANCED EDGE BASED ALGORITHM FOR THERMAL IMAGE SHARPENING

Martín I. Bayala ¹ & Raul E. Rivas ¹ & Raquel Niclos ²

¹ *Institute of Hydrology Plains (IHLLA), Scientific Research Commission of Buenos Aires Province (CIC), Pje. Arroyo Seco s/n, 7000, Tandil, Argentina.*

² *Earth Physics and Thermodynamics Department, University of Valencia, 50. Dr. Moliner, Burjassot, Valencia, Spain.*

Abstract. High temporal and spatial resolution thermal maps would significantly improve the assessment of the water content and crop productivity over a mixed agricultural landscape in the sub-humid Pampean Region of Argentina (PRA). However, the spatial resolution of the land surface temperature (LST) retrieved from sensors with high temporal resolution is not accurate enough to be used at crop field scale. Using the LST-Normalized Difference Vegetation Index (NDVI) relationship we developed a Difference of Edge model ($Ts*DL$) for downscaling coarse resolution thermal infrared (TIR) radiance to retrieve subpixel temperatures. The proposed technique was evaluated by comparing with the *DisTrad* Model, and validated by using ground dataset at local scales. The MODerate resolution atmospheric TRANsmission model (MODTRAN) was used with atmospheric profile data to atmospherically correct the Landsat 7 Enhanced Thematic Mapper (ETM) thermal band [2]. A Split Windows algorithm were applied to estimate LST image from EOS-MODIS TIR bands [3]. The results suggest that the $Ts*DL$ technique is the most adequate for simulating LST at high spatial resolution over heterogeneous landscapes, in agreement with the results shown in Bayala et al.(2013), the estimation error was less than 1 (°C).

Keywords. Downscaling, Thermal infrared, Landsat, MODIS.

1 Introduction

Land Surface Temperature (LST) is the most important input variable of energy budget and evapotranspiration models. The development of remote sensing (RS) techniques that provide support to monitor spatial LST variability at field-scale is required. However, the coarse satellite data, such as EOS-MODIS images, is not suitable for local-scale water and agricultural management applications. The hyperspectral MODIS and Landsat systems provide diverse land surface parameters such as LST and Vegetation Indices (VIs) at different spatial and temporal resolutions, which can be used to build an operative application to improve the LST mapping application at daily field and resolution with low cost. EOS-MODIS provides daily thermal infrared (TIR) and visible-near infrared (VNIR) band imagery at 1 km and 500-250 m spatial resolution respectively. The Landsat

7 ETM+ TIR band has a medium spatial resolution (60 m) and VNIR bands at 30 m, they are available every 16 days.

During last decade the LST-VIs relationship has been used to apply several sharpening empirical and semi-empirical models, such as the Disaggregation Procedure Results for Radiometric Surface Temperatures (DisTrad) [4]. This method use the empirical relationship between LST and NDVI defined by the negative slope variation generated in a linear fitting, allowing disaggregate a coarse spatial resolution LST image to fine spatial resolution.

The objective of this study was to evaluate the utility of the T_s^*DL in retrieving LST at high spatial resolution over agricultural area of the Pampean Region of Argentina.

2 Method

The T_s^*DL is define by the negative slope variation generated in a quadratic dry edge fitting and linear wet edge fitting between LST and NDVI(See Figure 1). The simulated dry (T_{SDELR}^*) and wet ($T_{SWE LR}^*$) edge LST images to high resolution can be expressed as:

$$T_{SDELR}^* = aVI_{LR}^2 + bVI_{LR} + c \quad (1)$$

$$T_{SWE LR}^* = aVI_{LR}^2 + b \quad (2)$$

The "star" symbol indicates a temperature value predicted by resulting regression equation over the dry and wet edges (Eq. 1 and Eq. 2). The "LR" and "HR" subscripts indicate that the images are at low and high spatial resolution respectively. The quadratic dry edge fitting parameters obtained at the coarse scale (Eq. 1) are then applied to the full-resolution VI data to simulate LST to a finer scale:

$$T_{SDLHR}^* = T_{SDEHR}^* + \Delta t + \Delta l \quad (3)$$

Where

$$\Delta t = LST_{LR} - T_{SDELR}^* \quad (4)$$

$$\Delta l = T_{SWE HR}^* - T_{SDEHR}^* \quad (5)$$

The divergence of the temperatures retrieved from the observed temperatures, which is caused by some non-vegetation factors, such as soil moisture variations, can be assessed at the coarse scale by Δt . The restoration of these residuals at the sharpened image is critical because it preserves spatial patterns in LST that are not accounted for by Eq. 1-2 [4]. Δl is the subtraction between the wet ($T_{SWE HR}^*$) and dry edge (T_{SDEHR}^*) LSTs simulated image based on Eq 1-2. The result is a high resolution image within each coarse-scale pixel that preserves the coherence in the radiometry of the original TIR band.

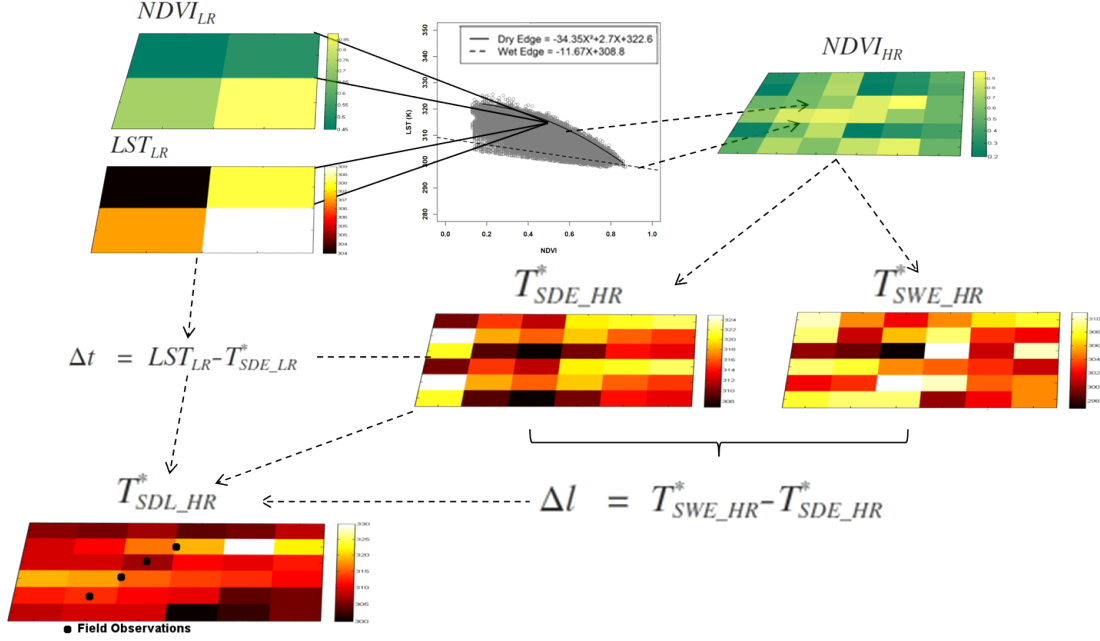


Figure 1: Flowchart of the T_{SDL} Methodology.

3 Data Used and Experimental Sites

Two Landsat ETM+ images (path/row: 228/82 and 225/86; see Table 1) with a spatial resolution of 30 m (VNIR) and 60 m (TIR) were utilized as reference data for model building and validation. Two calibrated TIRS and VNIR MODIS Terra bands at 1 km, 500 m and 250 m (MOD021km, MOD02HKM and MOD02QKM) and column water vapour (MOD05) products were used to retrieve the LST/VI images and downscaled by the proposed models. The EOS-MODIS dataset was matched spatially with the reference Landsat ETM+ data through common ground control points to reduce prediction errors due to spatial mismatch. The Landsat ETM+ LST was estimated by removing the effects of the atmosphere in the thermal region using MODTRAN radiative transfer code and the Planck equation [2]. The MODIS LST was obtained with the Split Window algorithm proposed in [3]. Two pairs of Landsat 7 ETM+ and EOS-MODIS Terra acquired on 12th February 2013 and 6th November 2013 were considered for applying downscaling techniques.

A statistical analysis of model performances was carried out for two different extensive rainfed agricultura areas on the PRA. The first validation site was located at Manfredi, Cordoba Province (MA, 32° 01' 25"S, 63° 41' 32"W) with prevalence of soybean cultivations and the second was located at Tandil, Buenos Aires Province (BA, 37° 17' 5"S, 58° 56' 37"W) with wheat cropland (See locations in Fig.2).

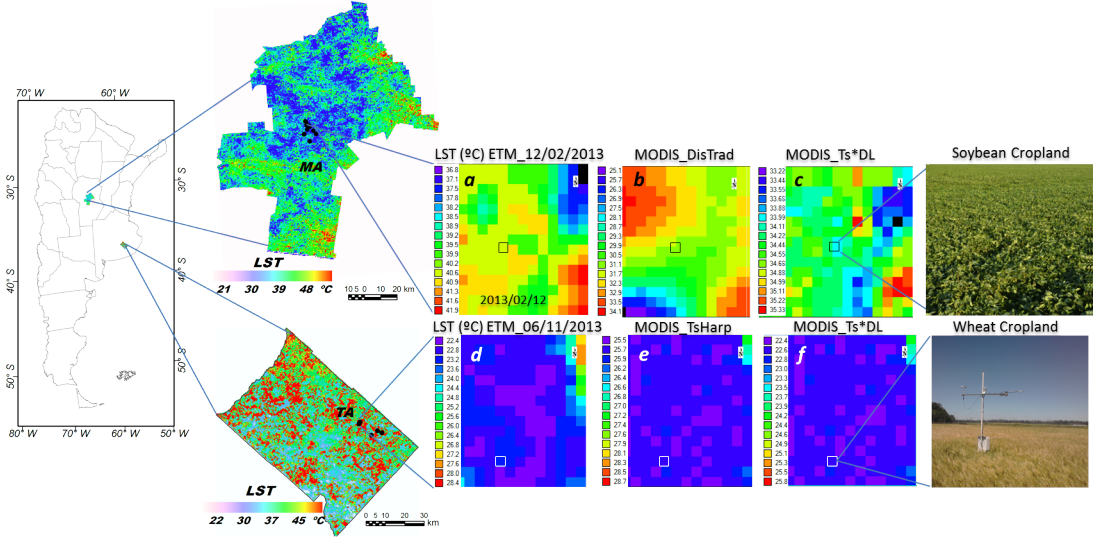


Figure 2: Validation sites in the PRA. (a), (d) are the Landsat ETM reference LST of 15 x 15 pixel window at 30 m. (b), (c), (e) and (f) are the MODIS downscaled images.

4 Quality Assessment

The ERGAS (Erreur Relative Globale Adimensionnelle de Synthèses) index was used to evaluate the statistical quality of the images sharpened at the Landsat ETM+ spatial resolution, it is independent of the units and resolution of the input image. Also, we assessed the following statistical parameters: Root Mean Square Error (RMSE), Spectrum Difference (SD) and Correlation Coefficient index (CC)[5]. The RMSE, ERGAS, SD and CC indices were perform such as:

$$RMSE = \sqrt{\sum_{i=1}^N (LST_{ref} - LST_{down})^2 / N} \quad (6)$$

$$ERGAS = 100 \frac{h}{l} \sqrt{\frac{1}{N} \sum_{i=1}^N \left(\frac{RMSE_i}{\bar{X}_{LST_{ref}}} \right)^2} \quad (7)$$

$$SD = \left| \frac{1}{N} \sum_{i=1}^M \sum_{j=1}^N \frac{LST_{ref} - LST_{down}}{LST_{ref}} \right| \quad (8)$$

$$CC = \frac{\sum_{i=1}^M \sum_{j=1}^N (LST_{ref} - LST_{ref}^{\bar{}})(LST_{down} - LST_{down}^{\bar{}})}{\sum_{i=1}^M \sum_{j=1}^N (LST_{ref} - LST_{ref}^{\bar{}})^2 (LST_{down} - LST_{down}^{\bar{}})^2} \quad (9)$$

where h is the resolution of the high LST spatial resolution image, l is the resolution of the low spatial resolution image, N is the number of spectral bands involved in the downscaling procedure, $RMSE_i$ is the root mean square error computed by Eq. 6, and $\bar{X}_{LST_{ref}}$ is the mean value of the reference LST image. LST_{ref} and LST_{down} are the reference and downscaled temperature. \bar{LST}_{ref} and \bar{LST}_{down} are the means of the reference and downscaled temperature.

The performance of the model can vary over various sensor image due to characteristics difference like wavelength, signal noise ratio, etc. Therefore, testing the models only on image may not be sufficient to comment on the models performance. Hence, the models were applied on real Landsat ETM+ and EOS-MODIS images and validated by means of ground dataset. Transects of ground LST measurements were carried out concurrently to the Landsat ETM+ and EOS-MODIS overpass times for each specific experimental site. Two types of thermal infrared radiometers were used for ground measurements: the CE 312 radiometer (CIMEL Electronique) with six bands (8-13 μm , 11.0-11.7 μm , 10.3-11.0 μm , 8.9-9.3 μm , 8.5-8.9 μm and 8.5-8.1 μm , respectively) and the SI-121 radiometer (Apogee instruments inc.) with one single band (8-14 μm). A blackbody calibration source was used before and after each measurement to check the radiometric performance. The ground measurements were emissivity corrected with data acquired with the Temperature Emissivity Separation (TES) method [6] and re-analysis atmospheric profiles from the National Centers for Environmental Prediction (NCEP) were used to estimate the atmospheric water vapour content involved in the atmospheric correction.

5 Result and Discussion

The study conducted during the crop growing period over Manfredi (MA) and Tandil (TA) test sites, are shown in the EOS-MODIS LST image at 240 m (Figure 2). Those images were obtained applying the downscaling techniques to target resolution of 960, 480 and 240 m (See Table 1). A subset of downscaled MODIS Terra and aggregated Landsat ETM to 240 m were statistically compared as shown in the Figure 3. A random sample of 5 % of the pixels were selected and extracted using the semivariogram technique, which the resulted R^2 were 0.8 and 0.9 and RMSE of 1.5 and 1.6, respectively.

Figure 4a-b present the residuals against fitted LST values (a) and quantile-quantile plots (b), in which high correlation between LST_{down} with respect to the normal line is indicate. However, the smallest and highest LST values are separate with respect to the normal line in (b) and zero (b), indicating pixels with high thermal variability due to the different proportions of bare soil and vegetation. This trend was observed for the two sharpening techniques.

The two sharpening models were tested on disaggregated Landsat ETM LST_{ref} image at NDVI resolution (30 m). A sub-scenes of 15 x 15 pixels of Landsat images taken on 12 February 2013 and 06 November 2013 were used as test data, they cover the areas of

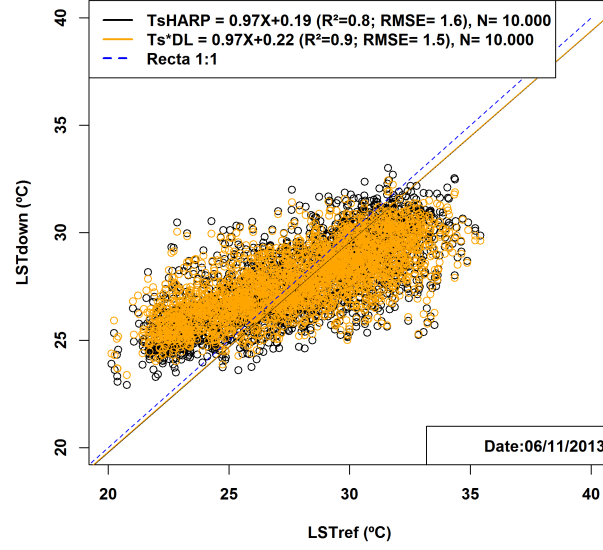


Figure 3: MODIS LST_{down} values obtained with two models vs. Landsat ETM+ LST_{ref} data.

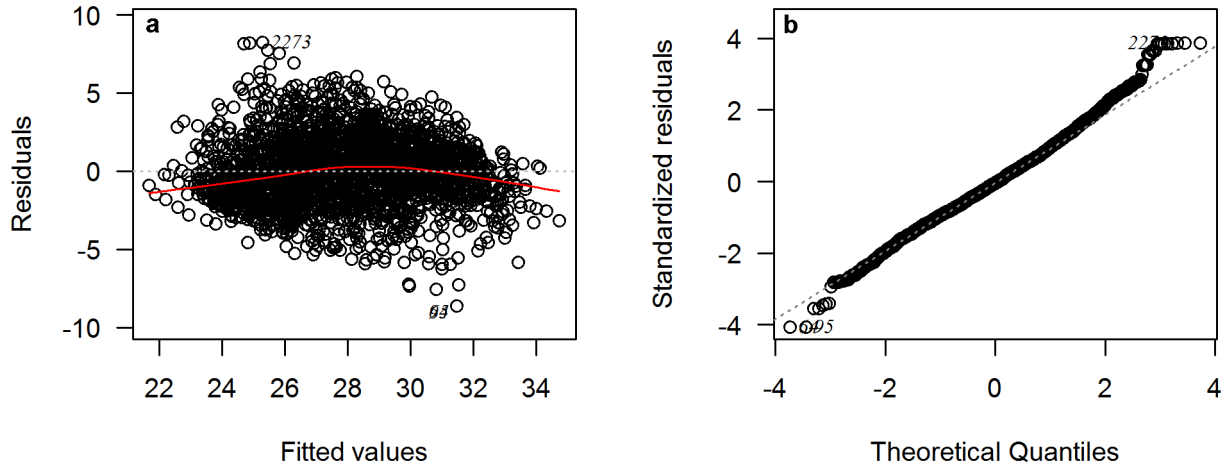


Figure 4: a)- Residuals vs. Fitted Ts^*DL values. b)- Normal Q-Q plot of Ts^*DL .

soybean and wheat fields (See Figure 2 (a),(b),(c),(d), (e) and (d)).

Table 1: LST_{ref} , LST_{down} , validation data with statistical results in $^{\circ}\text{C}$.

Site	Lat/Long	Date	Time (UTC)	LST Dataset	Mean	RMSE	ERGAS	CC	SD
MA	32° 01' 25" S 63° 41' 32" W	12/02/2013	13:58	ETM	40.3	-	-	-	-
			14:20	DisTrad	31.7	8.9	0.3	-0.1	0.0
			14:20	$Ts*DL$	34.1	6.2	0.2	0.5	0.0
			14:20	CE312	34.1 \pm 4	-	-	-	-
TA	37° 17' 5" S 58° 56' 37" W	06/11/2013	13:40	ETM	23.3	-	-	-	-
			14:45	DisTrad	25.9	2.7	1.5	0.7	0.1
			14:45	$Ts*DL$	22.7	1.0	0.5	0.7	0.0
			14:45	SI-121	22.2 \pm 2	-	-	-	-

The performance of two resampling methods is almost the same for rainfed soybean crop (Table 1), with ERGAS index of 0.3 (DisTrad) and 0.2 ($Ts*DL$). However, $Ts*DL$ was more accurate to represent the spatial patterns, the CC index value reached 0.5 for soybean crops. As shown in Figure 2 a-c, the spatial patterns in the test window of 15 x 15 pixel of the $Ts*DL$ image is similar to the LST_{ref} . Ground test data measured with CE312 radiometer showed the same average value of $Ts*DL$ method.

For wheat crop the performance was less accurate than the soybean crop, with ERGAS index of 1.5 and 0.5. Hence, the sharpening models were less accurate to preserve the spatial information over wheat crop (See Figure 2 d-e-f). However, The wheat field shows less RMSE than soybean crop, with 2.7 and 1 $^{\circ}\text{C}$. The data recorded by the sensor SI-121 is very similar to those obtained for LST_{ref} and LST_{down} image downsampled by the $Ts*DL$ model.

6 Conclusions

In this work, a TIR sharpening procedure with the same theoretical basis of the DisTrad model was proposed and evaluated over the PRA. The performance of the procedures was found to depend on the dry and wet edge definition in the LST-NDVI relationship. The results improved when using the quadratic function (dry edge), mainly because that function finds the maximum LST value where NDVI values are low.

The variation of soil moisture level affects downscaling model performance in different land cover classes. This determine the applicability of downscaling model in the agricultural and vegetated landscapes in the PRA.

The spectral and spatial quality of the downsampled images based on EOS-MODIS data have been evaluated quantitatively with statistical indices and ground dataset. The results confirm that the $Ts*DL$ model has higher spectral/spatial information preservation image compared with LST_{ref} .

References

- [1] Bayala, M.I., Rivas, R.E., Scavuzzo, M. (2013). *Generación de mapas de temperatura de alta resolución mediante técnicas de remuestreo*. Interciencia. 38, 502–508.
- [2] Barsi, J.A., Barker, J.L., Schott, J.R., 2003. An Atmospheric Correction Parameter Calculator for a Single Thermal Band Earth-Sensing Instrument. IGARSS03, Centre de Congres Pierre Baudis, Toulouse, France.
- [3] Coll, C., Caselles, V., Galve, J.M., Valor, E., Niclòs, R., Sanchez, J., Rivas, R. (2005). *Ground measurements for the validation of land surface temperatures derived from AATSR and MODIS data*. Remote Sensing of Environment, 97, 288-300.
- [4] Kustas, W.P., Norman, J.M., Anderson, M.C., French, A.N. (2003). *Estimating subpixel surface temperatures and energy fluxes from the vegetation index-radiometric temperature relationship*. Remote Sensing of Environment, 85, 429–440.
- [5] Zhan, W., Chen, Y., Zhou, J., Li, J., Liu, W. (2011). *Sharpening thermal imageries: a generalized theoretical framework from an assimilation perspective*. IEEE Trans. Geosci. Remote Sens. 49, 773-789.
- [6] Mira, M., Schmugge, T.J., Valor, E., Caselles, V., Coll, C. (2009). *Comparison of thermal infrared emissivities retrieved with the two-lid Box and the TES methods with laboratory spectra*. IEEE Trans. Geosci. Remote Sens., vol. 47, no. 4, pp. 1012-1021.